Wang *et al.*
Natural Products and Bioprospecting (2026) 16:42
https://doi.org/10.1007/s13659-026-00597-0

Natural Products and Bioprospecting

ORIGINAL ARTICLE Open Access

Phenazinoates A–E, five pairs of phenazine conjugates from a mangrove soil-derived *Streptomyces* strain OUCMDZ-4923

Dongyang Wang[1,3,4†], Peipei Liu[1†], Yukang Gao[1], Linmeng Chen[1], Liping Wang[3,4], Ning Li[5] and Weiming Zhu[1,2*]

Abstract

Phenazinoates A–E (**1**–**5**), comprising five pairs of methyl saphenate conjugates with genistein, *o*-aminophenol, *p*-acetaminophenol and glycerol, were isolated from the fermentation broth of mangrove soil-derived *Streptomyces* sp. OUCMDZ-4923. Their structures were determined through comprehensive one-dimensional and two-dimensional nuclear magnetic resonance spectroscopy, coupled with high-resolution electrospray ionization mass spectrometry. The absolute configurations of each isomer were established by comparing experimental electronic circular dichroism spectra with calculated counterparts. Based on the biosynthetic pathway analysis, compounds **1**–**3** were semi-synthesized from the reactions of methyl (*R*)-saphenate with genistein, *o*-aminophenol, and *o*-formamidophenol, utilizing microwave-assisted solid acid catalysis. The compounds were resolved as enantiomerically pure forms and subsequently tested for antibacterial efficacy against six pathogenic bacteria. Phenazinoates A (**1**) and B (**2**) demonstrated bioactivity against four Gram-positive bacterial strains, with minimum inhibitory concentration values ranging from 0.78 to 3.13 μg/mL.

Keywords Mangrove actinobacteria, *Streptomyces* sp., Phenazine conjugates, Structure elucidation, Antibacterial activity

†Dongyang Wang and Peipei Liu have contributed equally to this work.

*Correspondence:
Weiming Zhu
weimingzhu@ouc.edu.cn
Full list of author information is available at the end of the article

Springer

Graphical Abstract

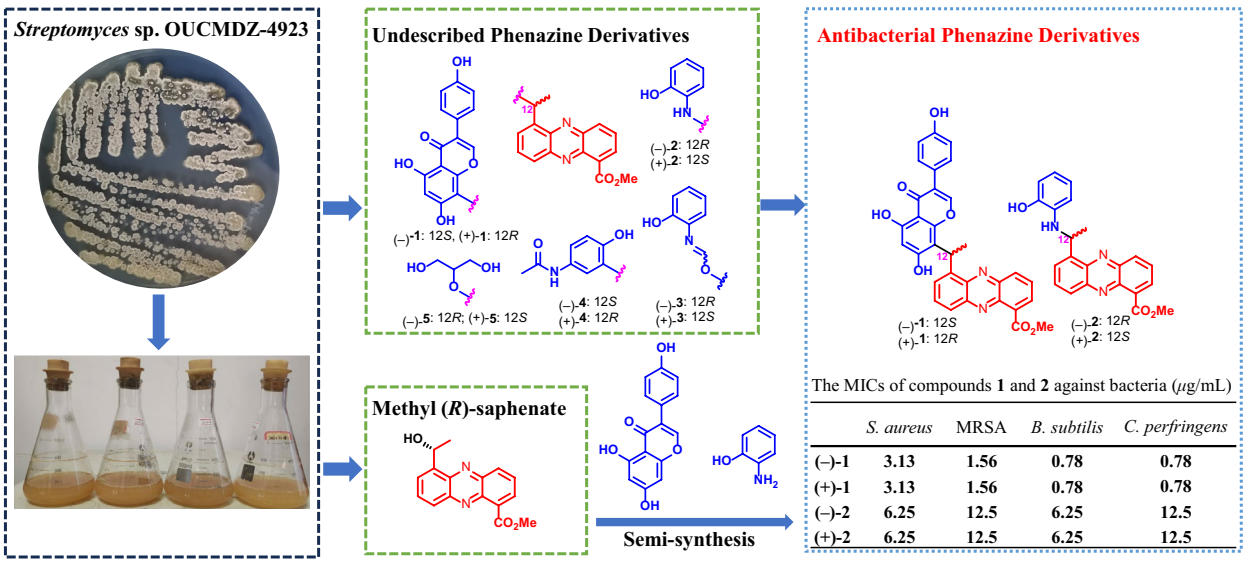

1 Introduction

Natural phenazine derivatives, primarily synthesized by species of *Pseudomonas* and *Streptomyces* [1–3], have been shown to exhibit a broad spectrum of biological activities. These include antibacterial [4, 5], antitumor [6, 7], anti-inflammatory [8, 9], and neuroprotective effects [10, 11]. Our previous work also discovered six phenazine derivatives that demonstrated notable cytotoxicity against tumor cells, potent antifungal activity against *Aspergillus fumigatus*, and activity against the H1N1 virus. These compounds were derived from the marine sponge-associated strain *Nocardiopsis dassonvillei* OUCMDZ-4534 [12]. In our ongoing exploration of bioactive phenazine derivatives of microbial origin, we have been particularly drawn to the untapped metabolic potential of soil-dwelling microorganisms, especially endophytes and their rhizosphere counterparts [13]. Within this context, we focused on a mangrove soil-derived actinobacterial strain, *Streptomyces* sp. OUCMDZ-4923, isolated from mangrove sediment closely associated with the roots of *Kandelia candel*. Bioinformatics analysis confirmed the presence of a phenazine biosynthetic gene cluster (*pnz*-BGC) in *Streptomyces* sp. OUCMDZ-4923 (GenBank accession No. CP170384), underscoring its potential to produce phenazine and its derivatives [14–16]. To pursue these bioactive compounds, a large-scale 60-L fermentation of *Streptomyces* sp. OUCMDZ-4923 was carried out. Chemical isolation of the ethyl acetate (EtOAc) extract resulted in the identification of sixteen enantiomerically pure phenazine dimers [16]. Further isolation efforts led to the discovery of five pairs of novel phenazine conjugates consisting of methyl saphenate linked with genistein, *o*-aminophenol, *p*-acetaminophenol and glycerol. These compounds were designated as phenazinoates A–E (**1**–**5**), along with the previously reported methyl (*R*)-saphenate (**6**) (Fig. 1) [16, 17]. Among the newly discovered compounds, phenazinoates A (**1**) and B (**2**), which are conjugates of genistein and *o*-aminophenol with methyl saphenate, demonstrated notable antibacterial activity against four strains of Gram-positive pathogenic bacteria, exhibiting minimum inhibitory concentration (MIC) values ranging from 0.78 to 3.13 μg/mL.

2 Results and discussion

2.1 Structural elucidation of phenazinoates A–E (1–5)

Phenazinoate A (**1**) was isolated as a racemic mixture in the form of a yellow powder. The molecular formula was established as $C_{31}H_{22}O_7N_2$ based on the high-resolution electrospray ionization mass spectrometry (HRESIMS) at *m*/*z* 535.1502 for the $[M+H]^+$ ion (calcd for $C_{31}H_{23}O_7N_2^+$, 535.1500). The UV–Visible absorption spectrum of the compound closely resembled those of known phenazine analogs, suggesting that the compound is indeed derivative of the phenazine family. The elucidation of the structure of compound **1** was further supported by the correlation spectroscopy (COSY) and heteronuclear multiple bond correlation (HMBC) experiments, as shown in Fig. 2. The COSY correlations revealed interactions from H-2 (δ_H 8.18) to H-4 (δ_H 8.23) through H-3 (δ_H 7.95), H-6 (δ_H 7.97) to H-8 (δ_H 8.06)

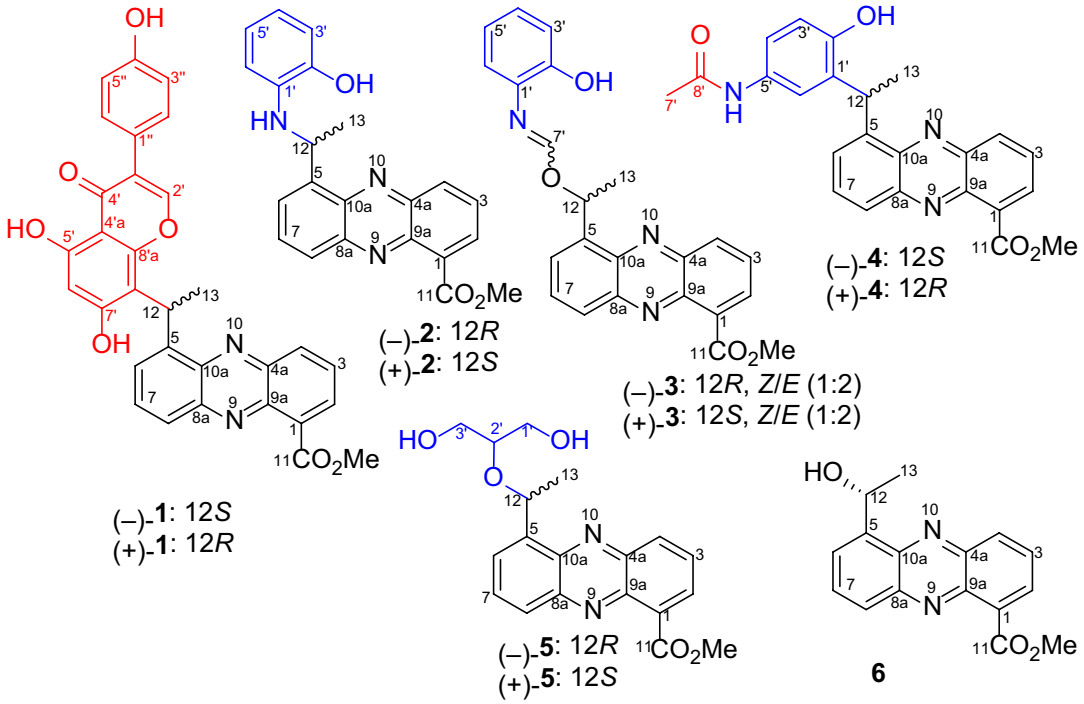

Fig. 1 The chemical structures of compounds **1**–**6**

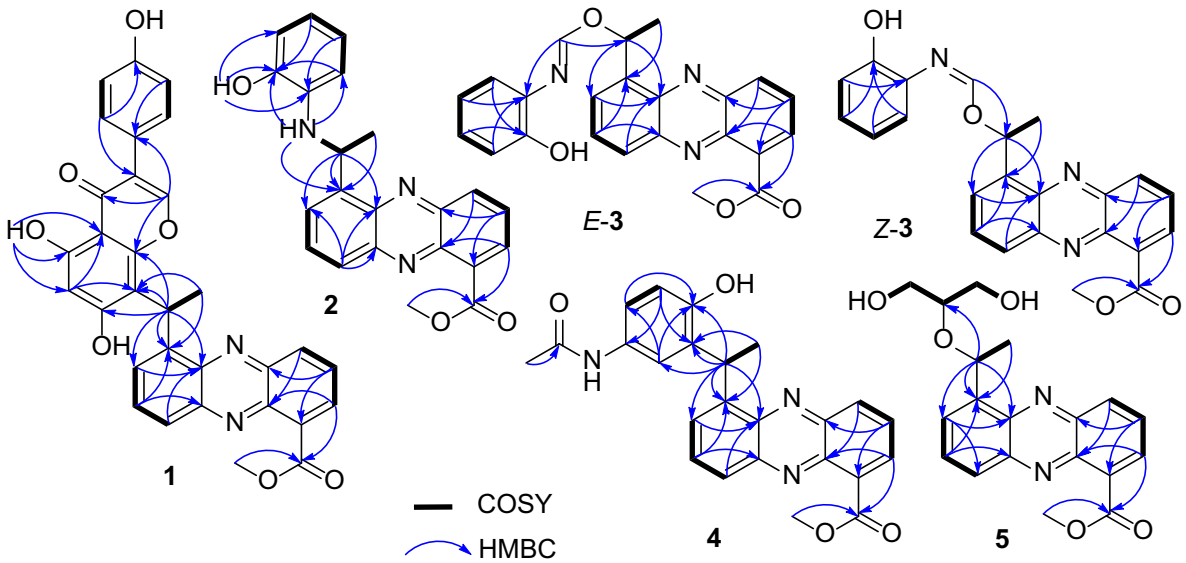

Fig. 2 Key COSY and HMBC correlations for the structural assignment of compounds **1**–**5**

through H-7 (δ_H 7.96), and between H-12 (δ_H 5.97) and H_3-13 (δ_H 1.90), indicating the presence of 5-ethylidenephenazine-1-yl moiety. Key HMBC correlations provided further structural insights. The coupling of H_3-13 to C-5 (δ_C 143.4), of H-12 to C-5, C-6 (δ_C 129.1), and C-10a (δ_C 141.6), as well as the interaction of the methoxy protons (δ_H 3.98) and H-2 with C-11 (δ_C 166.8), were indicative of a methyl 5-ethylidenephenazine-1-carboxylate moiety, akin to that found in methyl saphenate [17, 18]. Additionally, the ^{1}H and ^{13}C-NMR spectra hinted at the presence of an 8'-substituted genistein moiety within compound **1**. This was further corroborated by crucial HMBC correlations, including interactions from proton H-2' (δ_H 8.44) to C-4' (δ_C 180.3), C-8'a (δ_C 155.4), and

C-1" (δ_C 121.8). Moreover, the proton of the 5'-OH group (δ_H 13.02) exhibited correlations to C-4'a (δ_C 104.1), C-5' (δ_C 159.9), and C-6' (δ_C 99.4). H-6' (δ_H 6.20) also correlated with C-4'a and C-8' (δ_C 110.1). The observed ^{1}H-^{1}H COSY correlations between H-3"/5" (δ_H 6.82) and H-2"/6" (δ_H 7.39) further supported the structure of the genistein moiety. The attachment of the genistein structure to the phenazine core was confirmed through HMBC correlations from H_3-13 to C-8', and from H-12 to C-8', C-8'a, and C-7' (δ_C 164.4), indicating a single carbon–carbon bond connection between C-12 and C-8'. These NMR data and correlations provide compelling evidence for the structural integration of an 8'-substituted genistein moiety within the molecular architecture of the compound **1**, specifically methyl 5-(1-(genistein-8-yl)ethyl)-phenazine-1-carboxylate.

Phenazinoate B (**2**) was isolated as a racemic mixture and presented as a yellow powder. The molecular formula was determined to be $C_{22}H_{19}O_3N_3$, as indicated by the HRESIMS at *m/z* 374.1505 for the $[M+H]^+$ ion. Analysis of one-dimensional (1D) and two-dimensional (2D) NMR spectra, as detailed in Table 1 and Fig. 2, revealed that the structure includes a methyl 12-deoxysaphenate unit, similar to the structural component identified in previously discussed compound **1**. The spin system delineated by the chemical shifts from H-3' (δ_H 6.64) to H-6' (δ_H 6.17), passing through H-4' (δ_H 6.31) and H-5' (δ_H 6.33) in sequence, indicated the presence of an *ortho*-disubstituted phenyl group within the molecular structure. Critical HMBC interactions were observed, notably NH-12 (δ_H 5.38) showed correlations to C-5 (δ_C 144.1), C-2' (δ_C 144.3), and C-6' (δ_C 110.9). Additionally, the hydroxy proton HO-2' (δ_H 9.40) showed correlations with C-1' (δ_C 136.1), C-2', and C-3' (δ_C 113.7). These HMBC correlations confirmed the presence of an *o*-aminophenol moiety, which was connected to the C-12 atom via the amino nitrogen. Consequently, the molecular structure of phenazinoate B (**2**) was elucidated as methyl 5-(1-(2-hydroxyphenylamino)ethyl)phenazine-1-carboxylate.

Phenazinoate C (**3**) was isolated as a yellow powder, presenting a complex mixture that is both racemic and an inseparable mix of *E*/*Z*-isomers. Its molecular formula was determined to be $C_{23}H_{19}O_4N_3$ based on the HRESIMS peak at *m/z* 402.1456 for $[M+H]^+$ ion. When applying analytical high-performance liquid chromatography (HPLC) on an ND(2)-RH chiral column, it was feasible to separate compound **3** into enantiomerically pure entities, as illustrated in Fig. 3. The ^{1}H-NMR and distortionless enhancement by polarization transfer including the detection of quaternary nuclei (DEPTQ) spectra for compound **3** revealed two distinct sets of signals, with an approximate ratio of 2:1 when measured in pyridine-d_5. The structural elucidation of the major isomer within the mixture **3** began with the examination of its ^{1}H-NMR spin systems, as depicted in Fig. 2. The identification of a methyl 5-(1-alkoxyethyl)-phenazine-1-carboxylate moiety was substantiated by delineating three distinct spin systems: one extending from H-2 (δ_H 8.21) to H-4 (δ_H 8.38), a second from H-6 (δ_H 8.09) to H-8 (δ_H 8.30), and a third connecting H-12 (δ_H 7.28) to H_3-13 (δ_H 2.04). Additionally, pivotal HMBC interactions further clarified the structure, as illustrated in Fig. 2. Notable correlations including H_3-13 to C-5 (δ_C 141.3), H-12 to both C-5 and

Table 1 ^{1}H (500 MHz) and ^{13}C (125 MHz) NMR data for **1** and **2** in DMSO-d_6

No.	1		2	
	δ_H, mult. (*J* in Hz)	δ_C, type	δ_H, mult. (*J* in Hz)	δ_C, type
1		131.2, C		131.5, C
2	8.18, dd (1.4, 6.9)	131.7, CH	8.25, d (6.9)	131.9, CH
3	7.95, dd (6.9, 8.7)	129.6, CH	8.03, dd (6.9, 8.8)	130.0, CH
4	8.23, dd (1.4, 8.7)	132.5, CH	8.50, d (8.8)	132.9, CH
4a		140.8, C		141.1, C
5		143.4, C		144.1, C
6	7.97, dd (2.2, 7.0)	129.1, CH	7.93, dd (3.2, 6.9)	127.3, CH
7	7.96, dd (7.0, 7.8)	131.7, CH	7.92, t (6.9)	131.9, CH
8	8.06, dd (2.2, 7.8)	127.3, CH	8.08, dd, (3.2, 6.9)	128.0, CH
8a		142.9, C		143.1, C
9a		139.3, C		139.8, C
10a		141.6, C		141.0, C
11		166.8, C		166.9, C
12	5.97, q (7.3)	29.2, CH	5.80, dq (6.7, 7.9)	47.6, CH
13	1.90, d (7.3)	18.5, CH_3	1.68, d (6.7)	23.7, CH_3
11-OCH_3	3.98, s	52.5, CH_3	4.00, s	52.7, CH_3
12-NH			5.38, d (7.9)	
1'				136.1, C
2'	8.44, s	153.5, CH		144.3, C
3'		121.5, C	6.64, dd (2.1, 7.1)	113.7, C
4'		180.3, C	6.31, ddd (2.1, 7.1, 8.5)	116.2, CH
4'a		104.1, C		
5'		159.9, C	6.33, ddd (2.1, 7.1, 8.5)	119.6, CH
6'	6.20, s	99.4, C	6.17, dd (2.1, 7.1)	110.9, CH
7'		164.4[a], C		
8'		110.1, C		
8'a		155.4, C		
2'-OH			9.40, s	
1"		121.8, C		
2"/6"	7.39, d (8.7)	130.2, CH		
3"/5"	6.82, d (8.7)	115.1, CH		
4"		157.3, C		
5'-OH	13.02, s			

[a] Confirmed by HMBC correlations of H-12 and H-6' to the carbon at δ_C 164.4

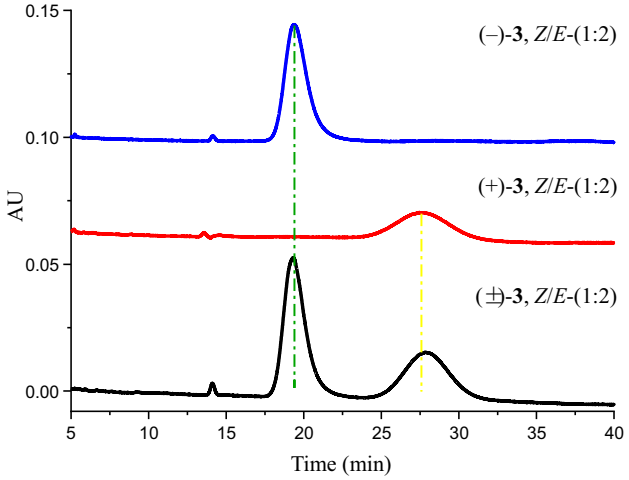

Fig. 3 The mixture **3** was resolved into optically pure compounds (–)-*Z*/*E*-**3** and (+)-*Z*/*E*-**3** using HPLC with a ND(2)-RH chiral column (4.6 × 250 mm) eluted with 45% MeCN-H_2O at 1 mL/min

C-6 (δ_C 129.7), as well as C-10a (δ_C 142.3). Correlations were also observed from both CH_3O-11 (δ_H 4.04) and H-2 to C-11 (δ_C 167.9). The presence of an *o*-aminophenol moiety within the structure of compound **3** was suggested by a set of COSY correlations, which traced the continuous connectivity from H-3' (δ_H7.16) to H-6' (δ_H 7.09). The structure was further elucidated by analyzing the HMBC cross-peaks. These revealed significant correlations from H-7' (δ_H 8.63) to C-12 (δ_C 51.0) and C-1' (δ_C 128.5), indicating the formation of a C=N bond between the 12-alkoxy group and the 1'-NH_2 group. These findings provided a clearer understanding of the compound's chemical constitution, identified as methyl 5-(1-((2-hydroxyphenylimino)methoxy)ethyl)phenazine-1-carboxylate. The structural assignment of the minor isomer of compound **3** was deduced to be the geometric isomer of its major counterpart, owing to the resemblance of their 2D NMR correlations, as presented in Fig. 2. The principal distinction arose from the 1D NMR data, particularly around the C=N moiety, detailed in Table 2. This assignment was further corroborated by the synthetic approach that involved combining methyl (*R*)-saphenate with *o*-formamidophenol or *o*-hydroxyphenyl formamide, which also aligned with the structural identification conclusions presented in Fig. 4a. Moreover, the fact that the mixture **3** remained an inseparable *E*/*Z*-isomeric blend was rationalized by the presence of a dynamic equilibrium between the *E*- and *Z*-geometric isomers in solution. This equilibrium is facilitated by two keto-enol tautomerizations, along with unrestricted rotation around the C-7'–N single bond, as depicted in Fig. 4b. These findings elucidated the dynamic behavior of the isomers and the complexity of their separation.

Table 2 ^1H (600 MHz) and ^{13}C (150 MHz) NMR data for **3** in pyridine-d_6

No.	3 (*E*- isomer, major)		3 (*Z*- isomer, minor)	
	δ_H, mult. (*J* in Hz)	δ_C, type	δ_H, mult. (*J* in Hz)	δ_C, type
1		133.0, C		133.1, C
2	8.21, dd (1.4, 6.9)	132.1, CH	8.23, dd (1.4, 6.9)	132.3, CH
3	7.76, dd (6.9, 8.7)	132.2, CH	7.77, dd (6.9, 8.7)	131.9, CH
4	8.38, dd (1.4, 8.7)	133.8, CH	8.38, dd (1.4, 8.7)	133.5, CH
4a		142.4, C		142.2, C
5		141.3, C		139.4, C
6	8.09, d (1.2, 6.9)	129.7, CH	7.64, d (6.9)	129.8, CH
7	7.77, dd (6.9, 8.7)	131.2, CH	7.72, dd (6.9, 8.7)	130.6, CH
8	8.30, dd (1.2, 8.7)	129.9, CH	8.34, dd (1.2, 8.7)	129.9, CH
8a		144.2, C		144.4, C
9a		141.1, C		141.2, C
10a		142.3 C		142.0, C
11		167.9, C		167.8, C
12	7.28, q (7.2)	51.0, CH	6.71, q (7.2)	52.8, CH
13	2.04, d (7.2)	19.1, CH_3	1.93, d (7.2)	19.1, CH_3
11-OCH_3	4.04, s	52.9, CH_3	4.05, s	52.9, CH_3
1'		128.5, C		125.6, C
2'		156.6, C		156.4, C
3'	7.16, dd (1.4, 8.0)	117.5, CH	7.13, d (8.0)	117.6, CH
4'	7.24, ddd (1.7, 8.0, 9.0)	130.1, CH	7.24, ddd (1.7, 8.0, 9.0)	130.1, CH
5'	6.83, ddd (1.4, 7.5, 9.0)	119.7, CH	6.82, dd (7.8, 9.0)	119.5, CH
6'	7.09, dd (1.7, 7.5)	131.9, CH	7.09, dd (1.7, 7.8)	131.5, CH
7'	8.63, s	164.3, CH	9.38, s	164.4, CH
2'-OH	12.00, s		11.31, s	

To ascertain the geometry of the C=N bond within the isomers of compound **3**, a Nuclear Overhauser Enhancement difference (NOEdiff) experiment was employed. The results, illustrated in Fig. 5, revealed distinct NOE correlations for each isomer. For the major geometric isomer of **3**, the NOE correlation observed between H-7' (δ_H 8.63) and H-6' (δ_H 7.09) allowed for the assignment of the *E*-geometry of the C=N bond Conversely, for the minor isomer of **3**, the selective irradiation of H-7' (δ_H 9.38) led to an enhancement observed at H-12 (δ_H 6.71), which indicated the *Z*-geometry of the C=N bond.

The racemic phenazinoate D (**4**) was isolated as a yellow powder. Its molecular formula, $C_{24}H_{21}O_4N_3$, was deduced from the HRESIMS peak at *m*/*z* 416.1604 $[M+H]^+$ (calcd for $C_{24}H_{21}N_3O_4^+$, 416.1605). The UV–Visible spectral data of the compound matched those of known phenazine analogs, indicating that **4** is a phenazine derivative. The inclusion of a methyl 5-(1-hydroxyethyl)-phenazine-1-carboxylate moiety was substantiated by pivotal 2D-NMR correlations, as

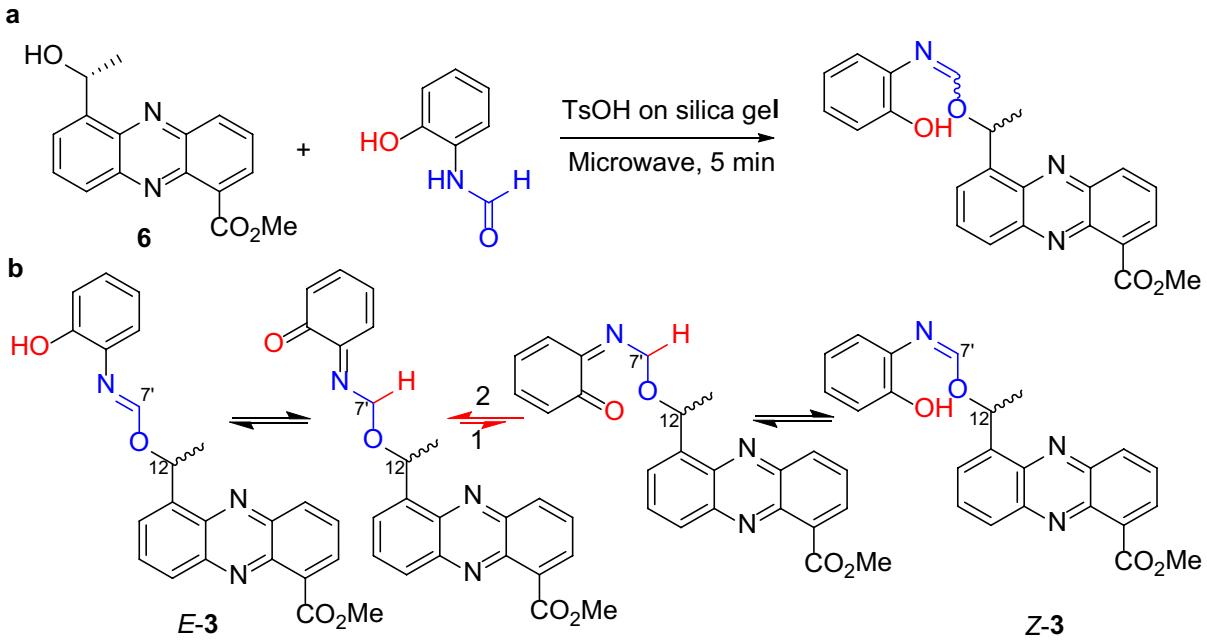

Fig. 4 The synthesis of **3** from **6** and *o*-formamidophenol (**a**). Possible *Z*/*E*- dynamic equilibrium in solution via keto-enol tautomerization and single bond rotation at C-7'; this dynamic allows for the interconversion between the *Z* and *E* isomers, contributing to the complexity of their separation and characterization (**b**)

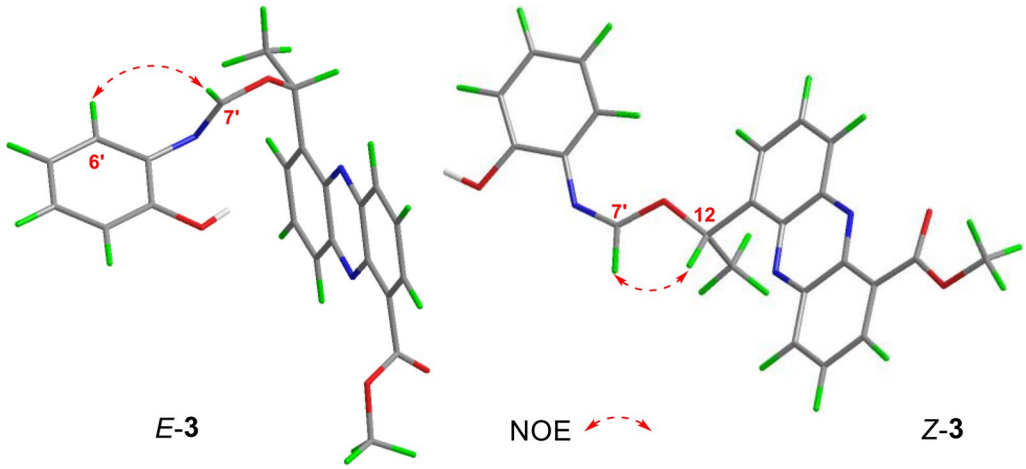

Fig. 5 NOE correlations of *Z*-**3** and *E*-**3**

depicted in Fig. 2. The structure features a 1',2',5'-trisubstituted phenyl ring, as evidenced by the COSY correlation of H-3' (δ_H 6.76) with H-4' (δ_H 7.01), as well as essential HMBC correlations. These include the coupling of H-3' to C-1' (δ_C 136.1) and C-5' (δ_C 126.2), H-4' to C-2' (δ_C 146.2) and C-6' (δ_C 121.7), and H-6' (δ_H 7.72) to both C-2' and C-4' (δ_C 123.8). Additionally, the pivotal HMBC signals connecting H-12 (δ_H 5.56) to C-1', C-2', and C-6' suggest that C-12 is directly bound to C-1' through a single C–C bond. The ^{1}H and ^{13}C NMR data (Table 3) revealed the presence of an additional methyl group at $\delta_{H/C}$ 2.03/23.5 (CH_3-7'), a carbonyl carbon at δ_C 169.0 (C-8'), and a phenolic hydroxy proton at δ_H 9.35. The HMBC correlations, specifically between H_3-7' and C-8', confirmed the presence of an acetamide moiety within the structure. The chemical shifts observed for C-2' and C-5' allowed for the definitive placement of the hydroxy and acetamide groups on the molecular framework. Consequently, the structures of these compounds were conclusively established

Table 3 ^{1}H and ^{13}C NMR data for compounds **4** and **5** in DMSO-d_6

No.	4 (600, 150 MHz)		5 (500, 125 MHz)	
	δ_H, mult. (*J* in Hz)	δ_C, type	δ_H, mult. (*J* in Hz)	δ_C, type
1		131.7, C		131.8, C
2	8.23, dd (1.4, 6.9)	131.4, CH	8.23, dd (1.4, 6.9)	131.3, CH
3	8.00, dd (6.9, 8.7)	129.8, CH	8.01, dd (6.9, 8.8)	129.9, CH
4	8.46, dd (1.4, 8.7)	132.9, CH	8.44, dd (1.4, 8.8)	132.7, CH
4a		141.2, C		141.1, C
5		145.8, C		143.3, C
6	7.77, d (7.0)	128.1, CH	8.20, d (6.8)	127.6, CH
7	7.96, dd (7.0, 8.7)	131.8, CH	8.03, dd (6.8, 8.8)	131.8, CH
8	8.07, dd (1.2, 8.7)	127.4, CH	8.14, dd (1.4, 8.8)	128.1, CH
8a		142.9, C		142.7, C
9a		139.6, C		139.6, C
10a		141.0, C		140.7, C
11		166.8, C		166.8, C
12	5.56, q (7.2)	36.7, CH	6.04, q (6.4)	70.2, CH
13	1.71, d (7.2)	21.5, CH_3	1.55, d (6.4)	23.8, CH_3
11-OCH_3	3.99, s	52.6, CH_3	4.00, s	52.6, CH_3
1′		136.1, C	3.45, ddd (5.3, 11.1, 16.5)	61.6, CH_2
			3.55, ddd (5.2, 11.4, 16.5)	
2′		146.2, C	3.37, dd (5.2, 5.3)	79.5, CH
3′	6.76, d (8.3)	115.9, CH	3.45, ddd (5.3, 11.1, 16.5)	60.8, CH_2
			3.55, ddd (5.2, 11.4, 16.5)	
4′	7.01, dd (2.1, 8.4)	123.8, CH		
5′		126.2, C		
6′	7.72, d (2.1)	121.7, CH		
7′	2.03, s	23.5, CH_3		
8′		169.0, C		
1′-OH			4.60, brs	
2′-OH	9.35, s			
3′-OH			4.60, brs	

as methyl 5-(1-(2-hydroxy-5-acetamidophenyl)ethyl) phenazine-1-carboxylate.

The racemic mixture of phenazinoate E (**5**) was obtained as a yellow powder and determined to have the molecular formula $C_{19}H_{20}O_5N_2$, as indicated by a HRESIMS peak at *m/z* 357.1451 $[M+H]^+$. The UV–Visible and ^{1}H,^{13}C-NMR spectral data for compound **5** suggested the presence of a methyl 5-(1-alkoxyethyl) phenazine-1-carboxylate moiety. The ^{1}H-^{1}H COSY correlations, as shown in Fig. 2, from HO-1′ (δ_H 4.60) to HO-3′ (δ_H 4.60) through H_2-1′ (δ_H 3.45/3.55), H-2′ (δ_H 3.37) and H_2-3′ (δ_H 3.45/3.55) in sequence indicated a glycerin fragment, with substitution occurring at the 2′-hydroxy position. The connection between the glycerin and phenazine units was implied by an ether linkage between C-12 and C-2′, supported by the HMBC correlation of H-2′ to C-12 (δ_C 70.2). Consequently, the structure of compound **5** was conclusively identified as methyl 5-(1-((1,3-dihydroxypropan-2-yl)oxy)ethyl) phenazine-1-carboxylate.

The new compounds **1**–**5** were successfully resolved into their optically pure enantiomers using HPLC equipped with chiral columns. To determine the absolute configurations (ACs) of these ten compounds, the electronic circular dichroism (ECD) curves for the (*R*)-isomers were computed using time-dependent density functional theory (TDDFT) with the B3LYP/6–31G(d) basis set [19, 20], as detailed in the Supporting Information. The comparison of the experimental ECD curves with the calculated ones for compounds (+)-**1**, (−)-**2**, (−)-**3**, (−)-**4**, and (−)-**5** showed a good correlation with the curves of their respective (*R*)-isomers, as illustrated in Fig. 6. Consequently, the ACs of compounds (+)-**1**, (−)-**2**, (−)-**3**, (+)-**4**, and (−)-**5** were assigned as (*R*)-, while the ACs of compounds (−)-**1**, (+)-**2**, (+)-**3**, (−)-**4**, and (+)-**5** were unambiguously determined to be (*S*)-.

2.2 Physicochemical properties of 1–5

2.2.1 Phenazinoate A (1)

Yellow powder; UV (MeOH) λ_{max} (log ε) 253 (3.65), 365 (2.87) nm; ^{1}H and ^{13}C NMR data (Table 1); HRESIMS *m/z* 535.1502 $[M+H]^+$ (calcd for $C_{31}H_{23}N_2O_7$, 535.1500). (−)-**1**, $[\alpha]_D^{28}$ −18.6 (*c* 0.1, MeOH); ECD (0.94 mM, MeOH) λ_{max} ($\Delta\varepsilon$) 251 (−11.7), 271 (+1.4) nm. (+)-**1**:$[\alpha]_D^{28}$ +14.7 (*c* 0.1, MeOH); ECD (0.94 mM, MeOH) λ_{max} ($\Delta\varepsilon$) 251 (+16.5), 272 (−1.6) nm.

2.2.2 Phenazinoate B (2)

Yellow powder; UV (MeOH) λ_{max} (log ε) 249 (2.93), 365 (2.17) nm; ^{1}H and ^{13}C NMR data (Table 1); HRESIMS *m/z* 374.1505 $[M+H]^+$ (calcd for $C_{22}H_{20}N_3O_3$, 374.1499). (−)-**2**, $[\alpha]_D^{28}$ −40.9 (*c* 0.1, MeOH); ECD (1.3 mM, MeOH) λ_{max} ($\Delta\varepsilon$) 209 (+14.4), 237 (+7.3), 254 (− 21.6) nm, 364 (−0.9). (+)-**2**, $[\alpha]_D^{28}$ +30.9 (*c* 0.1, MeOH); ECD (1.3 mM, MeOH) λ_{max} ($\Delta\varepsilon$) 209 (−14.0), 238 (−7.3), 254 (+21.6), 364 (+0.9) nm.

2.2.3 Phenazinoate C (3)

Yellow powder; UV (MeOH) λ_{max} (log ε) 251 (3.69), 365 (2.99) nm; ^{1}H and ^{13}C NMR data (Table 2); HRESIMS *m/z* 402.1456 $[M+H]^+$ (calcd for $C_{23}H_{20}N_3O_4$, 402.1488). (−)-**3**, $[\alpha]_D^{28}$ −37.1 (*c* 0.1, MeOH); ECD (1.2 mM, MeOH) λ_{max} ($\Delta\varepsilon$) 229 (−1.9), 250 (−5.1), 306 (−0.6). (+)-**3**, $[\alpha]_D^{28}$ +36.5 (*c* 0.1, MeOH); ECD (1.2 mM, MeOH) λ_{max} ($\Delta\varepsilon$) 229 (+2.1), 251 (+5.0), 307 (+0.6) nm.

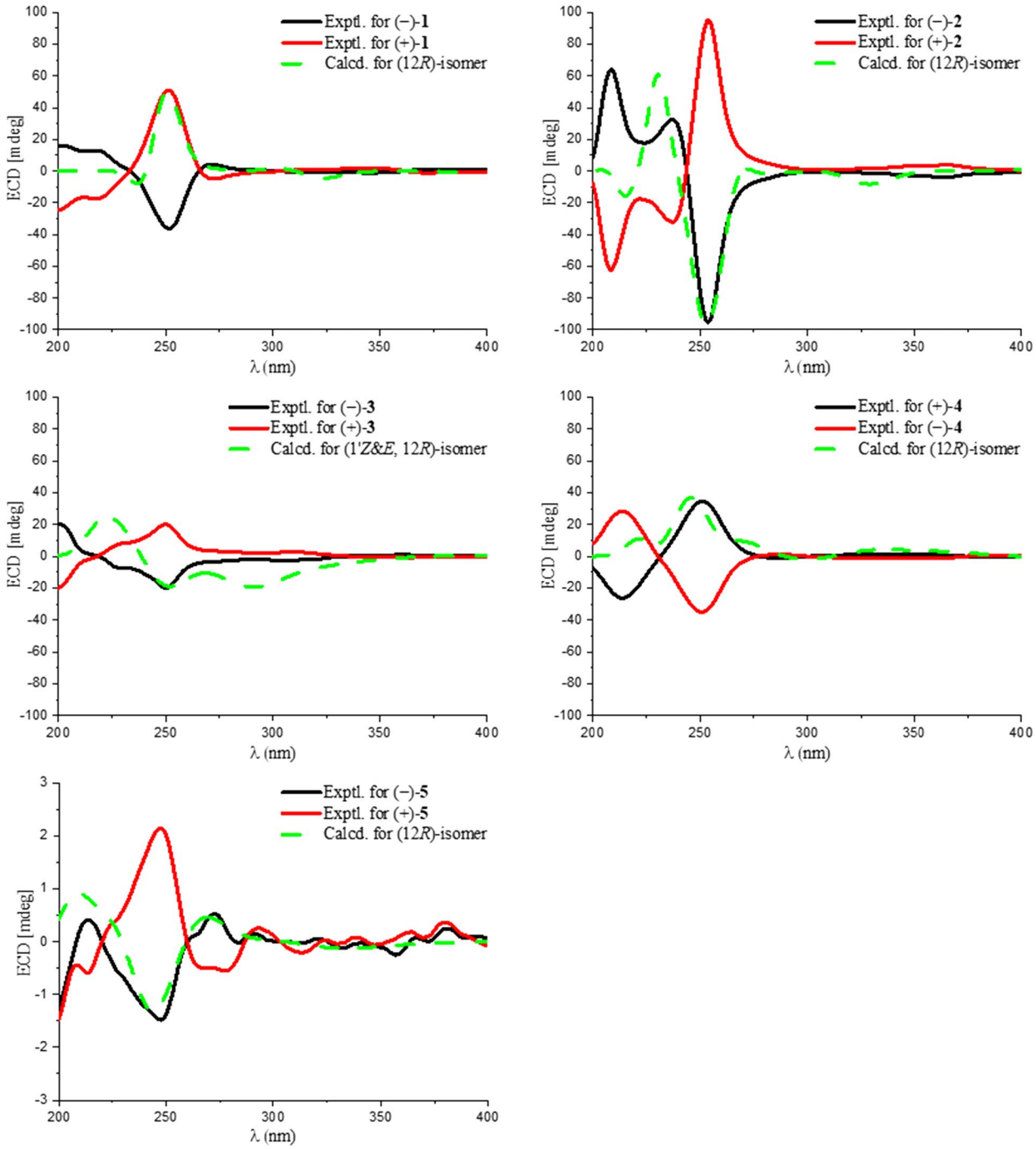

Fig. 6 The experimental and calculated ECD curves of **1**–**5**

2.2.4 Phenazinoate D (4)

Yellow powder; UV (MeOH) λ_{max} (log ε) 253 (3.46), 365 (2.77) nm; ^{1}H and ^{13}C NMR data (Table 3); HRESIMS *m/z* 416.1604 $[M+H]^+$ (calcd for $C_{24}H_{21}N_3O_4$, 416.1605). (−)-**4**, $[\alpha]_D^{28}$ −25.2 (*c* 0.1, MeOH); ECD (1.2 mM, MeOH) λ_{max} ($\Delta\varepsilon$) 214 (+7.2), 251 (−8.8), 286 (+0.3) nm. (+)-**4**, $[\alpha]_D^{28}$ +30.3 (*c* 0.1, MeOH); ECD (1.2 mM, MeOH) λ_{max} ($\Delta\varepsilon$) 214 (−6.6), 251 (+8.7), 284 (−0.2) nm.

2.2.5 Phenazinoate E (5)

Yellow powder; UV (MeOH) λ_{max} (log ε) 252 (3.60), 366 (2.86) nm; ^{1}H and ^{13}C NMR data (Table 3); HRESIMS

m/z 357.1451 $[M+H]^+$ (calcd for $C_{19}H_{21}N_2O_5$, 357.1445). (−)-**5**, $[\alpha]_D^{28}$ −9.3 (*c* 0.1, MeOH); ECD (1.4 mM, MeOH) λ_{max} ($\Delta\varepsilon$) 214 (+0.1), 248 (−0.3), 272 (+0.1) nm. (+)-**5**, [α]28 D + 9.6 (*c* 0.1, MeOH); ECD (1.4 mM, MeOH) λ_{max} ($\Delta\varepsilon$) 246 (+0.5), 272 (−0.1) nm.

2.3 Proposed biosynthetic pathway of compounds 1–5 and semi-synthetic production of compounds 1–3

Previously, we identified the enzymes Pnz16–21 in *Streptomyces* sp. OUCMDZ-4923 as being responsible for the biosynthesis of the phenazine-1,5-dicarboxylic acid core, which is consequently converted into (*R*)-saphenic acid by enzymes Pnz6–12 and then *O*-methylated to form methyl (*R*)-saphenate (**6**) by the methyltransferase Pnz43 [16]. We now propose that methyl 5-vinylphenazine-1-carboxylate, produced by the dehydration of methyl (*R*)-saphenate (**6**) under the action of enzymes Pnz28/30 [16], serves as a critical intermediate. This intermediate undergoes non-enzymatic reactions with compounds such as genistein, *o*-aminophenol, *o*-formamidophenol, *p*-acetamidophenol, and glycerol through a nonenzymatic pathway, leading to the formation of phenazinoates A–E (**1**–**5**) (Fig. 7). In line with this hypothesis, compounds **1**–**3** were successfully semi-synthesized from methyl (*R*)-saphenate (**6**) by reacting it with genistein, *o*-aminophenol, or *o*-formamidophenol. This transformation was achieved using *p*-toluenesulfonic acid absorbed on silica gel as a catalyst under microwave irradiation.

2.4 Biological activity evaluation of compounds 1–5

The antibacterial efficacy of five pairs of enantiomerically pure compounds **1**–**5** was assessed as previously described [21]. The panel of test pathogens included four Gram-positive bacteria: *Staphylococcus aureus* ATCC 6538, methicillin-resistant *S. aureus* ATCC 43300 (MRSA), *Clostridium perfringens* CGMCC 1.0876, and *Bacillus subtilis* CGMCC 1.3376, along with two Gram-negative bacteria: *Pseudomonas aeruginosa* ATCC 10145 and *Escherichia coli* ATCC 11775. The minimum inhibitory concentrations (MICs), which are the lowest concentrations that inhibit microbial growth, were determined across a range of 25.0–0.78 μg/mL. Compounds **1** and **2** exhibited inhibitory activity against *B. subtilis*, *C. perfringens*, *S. aureus*, and MRSA, with MIC values

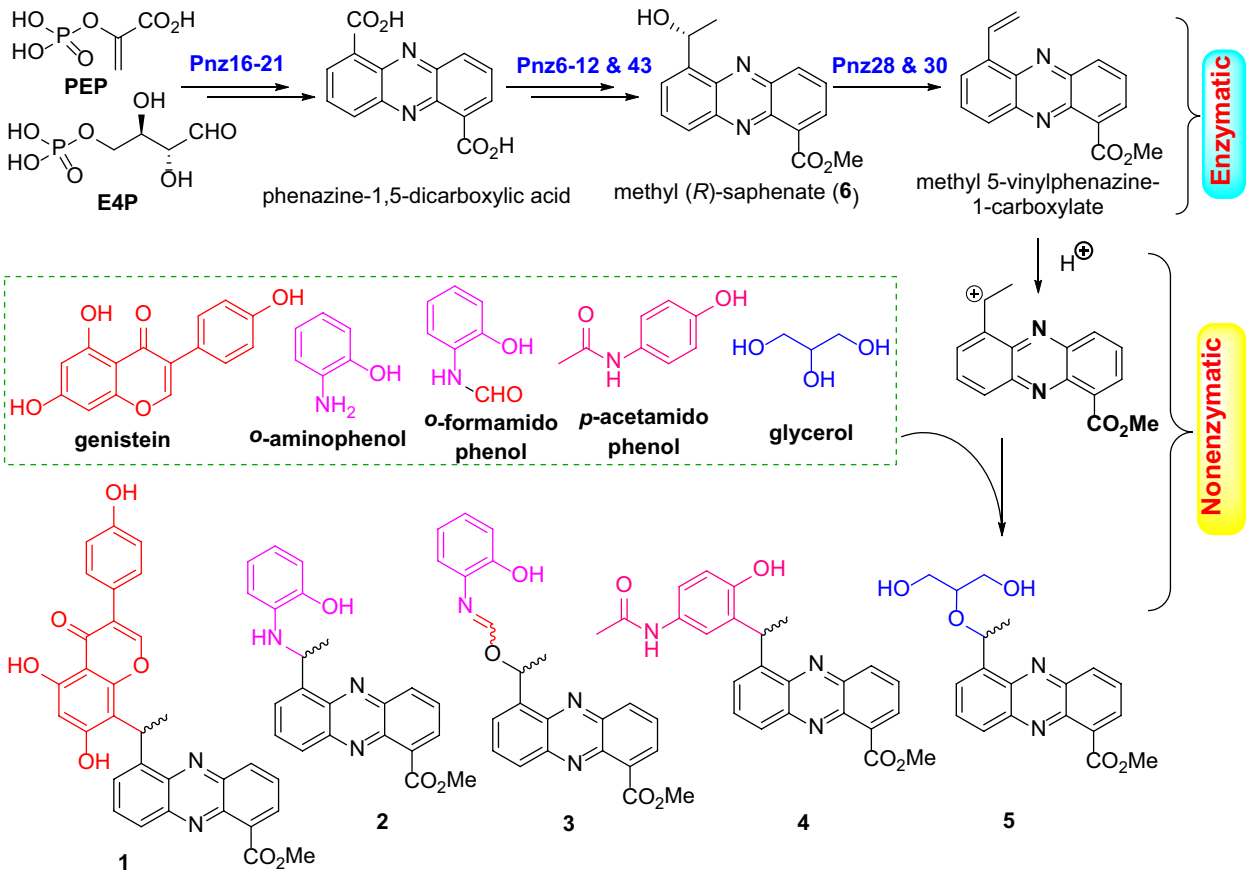

Fig. 7 Proposed biosynthetic pathway of phenazinoates **1**–**5** in *Streptomyces* sp. OUCMDZ-4923

ranging from 0.78 to 3.13 μg/mL, as detailed in Table 4. No antimicrobial activity was observed for the other tested bacteria, and compounds **3**–**5** did not exhibit inhibition against any of the test pathogens at the maximum concentration tested, which was 25.0 μg/mL. Additionally, it was noted that there was no difference in antibacterial activity between the two enantiomers. The results indicated that conjugating isoflavone or *o*-aminophenol moieties to the phenazine core can enhance the antibacterial efficacy of phenazine conjugates. However, both the *Levo-* and *Dextro-* enantiomers demonstrated the same level of efficacy against the four tested Gram-positive bacteria, suggesting that the chirality of these compounds does not influence their antibacterial activity. This observation could be explained by the possibility that the chiral center of the drug molecule may not located at the core position of the pharmacophore, or that the receptor's binding pocket is sufficiently spacious or flexible to accommodate either enantiomer, resulting in an equivalent biological effect.

3 Conclusion

In summary, five novel phenazine derivatives, phenazinoates A–E (**1**–**5**), were isolated and characterized from the mangrove soil-derived *Streptomyces* sp. OUC-MDZ-4923, representing five pairs of enantiomers. This marks the first study to report the conjugate of isoflavone, *o*-/*p*-aminophenol, or glycerol moieties to the phenazine core. Notably, compounds **1** and **2** which are conjugates of isoflavone or *o*-aminophenol and phenazine, exhibited antibacterial properties against a spectrum of four Gram-positive bacterial strains. Further insights were obtained from the analysis of biosynthetic pathways, leading to the successful semi-synthesis of phenazinoates A–C (**1**–**3**) from methyl (*R*)-saphenate using genistein, *o*-aminophenol, or *o*-acetamidophenol. This synthesis was facilitated by microwave-assisted solid acid catalysis, providing a method to produce these compounds in sufficient quantities for subsequent comprehensive studies on their antibacterial activities.

Table 4 The MICs of compounds **1** and **2** against bacteria (μg/mL)[a]

Compounds	*S. aureus*	MRSA	*B. subtilis*	*C. perfringens*
(–)-**1**	3.13	1.56	0.78	0.78
(+)-**1**	3.13	1.56	0.78	0.78
(–)-**2**	6.25	12.5	6.25	12.5
(+)-**2**	6.25	12.5	6.25	12.5
Cip[b]	0.098	0.39	0.012	0.049

[a] The MICs for compounds **3**–**5** against *B. subtilis*, *C. perfringens*, *S. aureus*, MRSA, *P. aeruginosa*, and *E. coli* as well as those for compounds **1** and **2** against *P. aeruginosa*, and *E. coli*, were all greater than 25.0 μg/mL

[b] Ciprofloxacin hydrochloride, used as the positive control, exhibited MICs of 0.049 μg/mL against *P. aeruginosa* and 0.0061 μg/mL against *E. coli*, respectively

Supplementary Information

The online version contains supplementary material available at https://doi.org/10.1007/s13659-026-00597-0.

Supplementary material 1.

Acknowledgements
This work was financially supported by the National Key Research and Development Program of China (No. 2022YFC2804100), the National Natural Science Foundation of China (No. 82473838), and Guizhou Provincial Basic Research Program (Natural Science) (No. QKHJC MS[2025]117).

Author contributions
D. Wang performed the experiments and wrote the draft paper, P. Liu participated in the experiments, Y. Gao and L. Chen analyzed the data and discussed the result, L. Wang and N. Li reviewed the manuscript, and Weiming Zhu conceived the projects, revised manuscript, and provided financial support. All authors read and approved the final manuscript.

Data availability
The datasets used or analyzed during the current study are available from the corresponding author on reasonable request.

Declarations

Competing interests
The authors declare no competing interests.

Author details
[1]Key Laboratory of Marine Drugs, School of Medicine and Pharmacy, Ministry of Education of China, Ocean University of China, Qingdao 266003, China. [2]Laboratory for Marine Drugs and Bioproducts, Qingdao Marine Science and Technology Center, Qingdao 266237, China. [3]Natural Product Research Center of Guizhou Province, Guiyang 550014, China. [4]State Key Laboratory of Discovery and Utilization of Functional Components in Traditional Chinese Medicine, Guizhou Medical University, Guiyang 550014, China. [5]Biology Institute, Engineering Research Center of Zebrafish Models for Human Diseases and Drug Screening of Shandong Province, Qilu University of Technology (Shandong Academy of Sciences), Jinan 250103, China.

Received: 4 November 2025 Accepted: 26 January 2026
Published online: 04 March 2026

References

1. Byng GS, Eustice DC, Jensen RA. Biosynthesis of phenazine pigments in mutant and wild-type cultures of *Pseudomonas aeruginosa*. J Bacteriol. 1979;138:846–52. https://doi.org/10.1128/jb.138.3.846-852.1979.
2. McDonald M, Wilkinson B, Van'T Land CW, Mocek U, Lee S, Floss HG. Biosynthesis of phenazine antibiotics in *Streptomyces antibioticus*: stereochemistry of methyl transfer from carbon-2 of acetate. J Am Chem Soc. 1999;121:5619–24. https://doi.org/10.1021/ja991159i.
3. Laursen JB, Nielsen J. Phenazine natural products: biosynthesis, synthetic analogues, and biological activity. Chem Rev. 2004;104:1663–86. https://doi.org/10.1021/cr020473j.
4. Kitahara M, Nakamura H, Matsuda Y, Hamada M, Naganawa H, Maeda K, et al. Saphenamycin, a novel antibiotic from a strain of *streptomyces*. J Antibiot. 1982;35:1412–4. https://doi.org/10.7164/antibiotics.35.1412.
5. Liang Y, Chen L, Ye X, Anjum K, Lian XY, Zhang Z. New streptophenazines from marine *Streptomyces* sp. 182SMLY. Nat Prod Res. 2017;31:411–7. https://doi.org/10.1080/14786419.2016.1169419.

6. Conda-Sheridan M, Marler L, Park EJ, Kondratyuk TP, Jermihov K, Mesecar AD, et al. Potential chemopreventive agents based on the structure of the lead compound 2-bromo-1-hydroxyphenazine, isolated from *Streptomyces* species, strain CNS284. J Med Chem. 2010;53:8688–99. https://doi.org/10.1021/jm1011066.
7. Moris M, Andrieu C, Rocchi P, Seillan C, Acunzo J, Brunel F, et al. 2,3-Dialkoxyphenazines as anticancer agents. Tetrahedron Lett. 2015;56:2695–8. https://doi.org/10.1016/j.tetlet.2015.04.003.
8. Kondratyuk TP, Park EJ, Yu R, van Breemen RB, Asolkar RN, Murphy BT, et al. Novel marine phenazines as potential cancer chemopreventive and anti-inflammatory agents. Mar Drugs. 2012;10:451–64. https://doi.org/10.3390/md10020451.
9. Lee HS, Kang JS, Choi BK, Lee HS, Lee YJ, Lee J, et al. Phenazine derivatives with anti-Inflammatory activity from the deep-sea sediment-serived yeast-like fungus *Cystobasidium laryngis* IV17-028. Mar Drugs. 2019;17:482. https://doi.org/10.3390/md17080482.
10. Kim WG, Ryoo IJ, Yun BS, Shin-ya K, Seto H, Yoo ID. Phenazostatin C, a new diphenazine with neuronal cell protecting activity from *Streptomyces* sp. J Antibiot. 1999;52:758–61. https://doi.org/10.7164/antibiotics.52.758.
11. Kim WG, Ryoo IJ, Yun BS, Shin-ya K, Seto H, Yoo ID. New diphenazines with neuronal cell protecting activity, phenazostatins A and B, produced by *Streptomyces* sp. J Antibiot. 1997;50:715–21. https://doi.org/10.7164/antibiotics.50.715.
12. Liu H, Zhu G, Zhao S, Fu P, Zhu W. Bioactive natural products from the marine sponge-derived *Nocardiopsis dassonvillei* OUCMDZ-4534. Chin J Org Chem. 2019;39:507–14. https://doi.org/10.6023/cjoc201806045.
13. Wang D, Li M, Xu Y, Fu P, Zhu W, Wang LP. Dibohemamines I–O from *Streptomyces* sp. GZWMJZ-662, an endophytic actinomycete from the medicinal and edible plant *Houttuynia cordata* Thunb. Nat Prod Bioprospect. 2025;15:9. https://doi.org/10.1007/s13659-024-00494-4.
14. Bauman KD, Li J, Murata K, Mantovani SM, Dahesh S, Nizet V, et al. Refactoring the cryptic streptophenazine biosynthetic gene cluster unites phenazine, polyketide, and nonribosomal peptide biochemistry. Cell Chem Biol. 2019;26:724-736.e7. https://doi.org/10.1016/j.chembiol.2019.02.004.
15. Rui Z, Ye M, Wang S, Fujikawa K, Akerele B, Aung M, et al. Insights into a divergent phenazine biosynthetic pathway governed by a plasmid-born esmeraldin gene cluster. Chem Biol. 2012;19:1116–25. https://doi.org/10.1016/j.chembiol.2012.07.025.
16. Wang D, Liu P, Xia Y, Wang L, Li N, Zhu W. Antibacterial dimeric phenazine derivatives from a marine-derived *Streptomyces* sp. OUCMDZ-4923. Mar Life Sci Technol. 2025;7:925–36. https://doi.org/10.1007/s42995-025-00328-3.
17. Geiger A, Keller-Schierlein W, Brandl M, Zähner H. Metabolites of microorganisms. 247. Phenazines from *Streptomyces antibioticus*, strain TUE 2706. J Antibiot. 1988;41:1542–51. https://doi.org/10.7164/antibiotics.41.1542.
18. Yun B, Ryoo I, Kim W, Kim J, Koshino H, Seto H, et al. Structures of phenazostatins A and B, neuronal cell protecting substances of microbial origin. Tetrahedron Lett. 1996;37:8529–30. https://doi.org/10.1016/0040-4039(96)01983-1.
19. Du Y, Chen Z, Li H, Wang Y, Fu P, Zhu W. Pafuranones A and B, two dimeric polyketides from a rare marine algae-derived fungus *Paraconiothyrium* sp. Chin Chem Lett. 2019;30:981–4. https://doi.org/10.1016/j.cclet.2019.01.034.
20. Zhu G, Kong F, Wang Y, Fu P, Zhu W. Cladodionen, a cytotoxic hybrid polyketide from the marine-derived *Cladosporium* sp. OUCMDZ-1635. Mar Drugs. 2018;16:71–8. https://doi.org/10.3390/md16020071.
21. Wang D, Wang C, Gui P, Liu H, Khalaf SMH, Elsayed EA, et al. Identification, bioactivity, and productivity of actinomycins from the marine-derived *Streptomyces heliomycini*. Front Microbiol. 2017;8:1147. https://doi.org/10.3389/fmicb.2017.01147.

Publisher's Note